Optimization of TiN-based ultra-flexible materials for photothermal and solar harvesting applications

Journal of Physics: Conference Series **2485** (2023) 012003 doi:10.1088/1742-6596/2485/1/012003

Optimization of TiN-based ultra-flexible materials for photothermal and solar harvesting applications

Do T. Nga[1], Thudsaphungthong Julie[2], Chu Viet Ha[2], Chu Thuy Anh[1], Do Chi Nghia[3] and Anh D. Phan[4]

[1] Institute of Physics, Vietnam Academy of Science and Technology, 10 Dao Tan, Ba Dinh, Hanoi, Vietnam
[2] Faculty of Physics, Thai Nguyen University of Education, Thai Nguyen, Vietnam
[3] Hanoi Pedagogical University 2, Nguyen Van Linh Street, Vinh Phuc, Vietnam
[4] Faculty of Materials Science and Engineering, Phenikaa University, Hanoi, Vietnam

E-mail: dtnga@iop.vast.vn

Abstract. We propose a theoretical model to investigate photothermal heating of ultra-flexible metamaterials, which are obtained by randomly mixing TiN nanoparticles in polydimethylsiloxane (PDMS). Due to the plasmonic properties of TiN nanoparticles, incident light can be perfectly absorbed in a broadband range (300-3000 nm) to generate heat within these metamaterials. Under irradiation of an 808 nm near-infrared laser with different intensities, our predicted temperature rises as a function of time agree well with recent experimental data. For a given laser intensity, the temperature rise varies non-monotonically with the concentration of TiN nanoparticles. Increasing the TiN concentration leads to a decrease in the heating process since the thermal conductivity grows. A small TiN concentration significantly reduces the absorbed energy and, thus, the system is less heated. When we apply this model to solar heating, we find that the temperature rise is no longer non-monotonic, and the heating efficiency is much lower than in the laser case. Our studies would provide good guidance for future experimental studies on the photothermal heating of broadband perfect absorbers.

1. Introduction

Nowadays, people have found plasmonic nanostructures interesting since they have various applications in different fields such as photothermal medical treatment [1, 2], energy harvesters and storage [3, 4, 5], image resolution enhancement [6, 7], and sensors to detect matters and small change of properties [8]. Due to a large number of free electrons on the surface of plasmonic materials, they can interact with incident light via light-induced excitation of collective electrons. The collective dynamics triggers optical resonances, so-called plasmon resonances. The plasmonic properties are strongly dependent on environment, size, shape, separation distance among nanostructures since these factors change local density of electrons on the surface [9, 10]. Thus, there are a variety of structures can be proposed and designed for a specific applications. It is essential to have theoretical models to optimize plasmonic nanostructures to be suitable with desired applications.

There are several types of plasmonic materials. Noble metals are conventional plasmonic materials are which are higly active and durable. Disadvantages of novel metals are expensive and unstable when operating at high temperatures. For these reasons, it is very hard to fabricate

plasmonic devices in mass production. One of new types of plasmonic materials, which has recently emerged, is 2 dimensional (2D) materials such as graphene, MoS_2, ... Researchers all over the world have exploited these 2D materials to design flexible and wearable devices. However, the number of free electrons in 2D materials are much smaller than that in noble metals. Thus, most applications have been towards mid-infrared and higher-wavelength regime. Another types of plasmonic materials are oxides and nitrides. They are known as alternative plasmonic materials, which can replace conventional plasmonic materials in a wide range of applications [11, 12].

Among metal nitrides, TiN has been intensively investigated because its optical properties are found to behave the same manner as gold's [13, 14, 15]. However, advantages of TiN are much cheaper and easier to fabricate than gold-based devices [11, 12]. Furthermore, TiN can be melt at 2930 ^{0}C, which is much higher than the melting temperature of gold (1064 ^{0}C). This feature leads to thermodynamic stability and high temperature operating capability. However, the dielectric function of TiN is sensitive to processing conditions [16]. Thus, optical properties of TiN-based devices can be changed.

Recently, designing metamaterials by mixing plasmonic nanoparticles with fiber or polymer has been a tropical topic in scientific and industrial applications [17, 18], The engineered materials are found to have broadband perfect absorption and they are ultraflexible. These ultraflexible metamaterials definitely overcome disadvantages of the rigid counterparts and can be exploit in multifunctional applications, particularly solar energy harvesters and photo-to-thermal converters. There are many variables to control photothermal performance of these applications. Proposing an effective approach to optimize the photothermal features is really needed. An obvious approach is to use finite-element simulations to understand temporal and spatial temperature variation [17]. However, complications of boundary conditions and inability to tune many assumptions in commercial softwares limit their applications to compare quantitatively with experiments and real a true nature. Commercial softwares are also expensive and hardly accessed by scientists in low-income countries. Using theoretical approaches are necessary and reasonable since they are simple, cheap, and modifiable, and have clear physical assumptions.

In this work, we apply the proposed model in Ref. [18] to describe photothermal experiments on TiN-based ultra-flexible metamaterials in Ref. [17]. First, we calculate spatial and temporal distributions of temperature under laser illumination and compare theoretical predictions with experiments. Form this, the validation of our approach is confirmed and discussed. Then, we vary the particle density to understand how the temperature increase is affected. Nonmonotonic variation of the temperature rise clearly suggests us how to optimize the photothermal heating, Finally, the model is extended to investigate the heating process of the ultraflexible metamaterials under solar irradiation.

2. Theoretical background

In this section, we use theoretical models to describe photothermal effects in flexible metamaterials composed of a random mixture of TiN nanoparticles embbeded in polymer PDMS (as shown in Fig. 1) and optimize the light-induced temperature rise of the systems. The flexible metamaterials have been fabricated in a recent experimental work [17]. The radius of TiN nanoparticles is fixed at 30 nm to mimic experiments in Ref. [17]. Light absorption of TiN nanoparticles heats up the nanostructures and thermally dissipates into their surrounding medium. Thus, temperature of our TiN-based metamaterials is increased.

In several prior works [19, 20], we used a heat energy balance equation to formulate expression for spatial distributions of laser-induced temperature rise of semi-infinite substrate. The

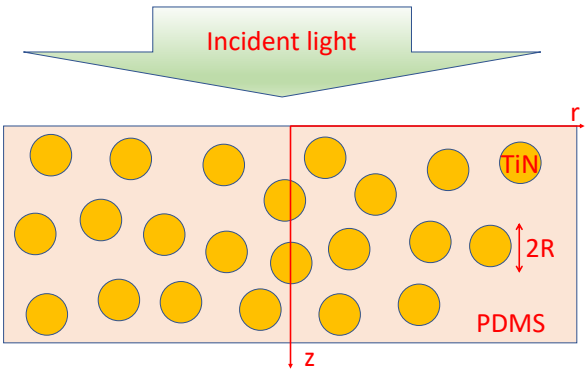

Figure 1. (Color online) Illustration of TiN-based ultra-flexible metamaterials including a random mixture of the plasmonic nanoparticles in PDMS under irradiation of incident light (laser/solar light).

expression is

$$\Delta T(r,z,t) = \frac{I_0(1-\mathcal{R})\alpha}{2\rho_d c_d}\int_0^t \exp\left(-\frac{\beta^2 r^2}{1+4\beta^2\kappa t'}\right)\frac{e^{\alpha^2\kappa t'}}{1+4\beta^2\kappa t'}\times \\ \times\left[e^{-\alpha z}\mathrm{erfc}\left(\frac{2\alpha\kappa t'-z}{2\sqrt{\kappa t'}}\right)+e^{\alpha z}\mathrm{erfc}\left(\frac{2\alpha\kappa t'+z}{2\sqrt{\kappa t'}}\right)\right]dt', \quad (1)$$

where I_0 is the laser intensity, c_d is the specific heat capacity, ρ_d is the mass density, α is the absorption coefficient at the wavelength λ of incident light, z and r are the depth direction and the radial distance, which are perpendicular and parallel to the metamaterial surface, respectively, as defined in Fig. 1, $\mathcal{R}$ is the reflectivity, β is the inverse of the laser spot radius [17], and $\kappa = K_d/\rho_d c_d$ is the thermal diffusivity. According to experimental results in Ref. [17], the metamaterial is a perfect absorber and, thus, $\mathcal{R} \approx 0$ and $1/\beta = 2$ cm.

The absorption coefficient α is strongly dependent on optical properties of nanoparticles and the dielectric function. Extinction spectra of spherical nanoparticles having the radius R in a medium can be theoretically calculated using Mie theory [19, 21]. For many years [19, 21], Mie calculations have exhibited a good agreement with experiments and simulation for a wide range of materials and sizes. However, the theoretical approach is valid when concentration solutions of nanoparticles are low and the plasmonic coupling among particles is ignored. The plasmonic coupling dramatically modifies electromagnetic fields surrounding the spherical particles and make it spherical asymmetry. In this work, we only consider the flexible metamaterials having low particle density. The Mie extinction cross section of a TiN nanoparticle in PDMS can be written as

$$Q_{ext} = \frac{2\pi}{x^2}\sum_{n=1}^{\infty}(2n+1)Re\left(a_n+b_n\right), \quad (2)$$

where

$$a_n = \frac{m^2 j_n(mx)\left[xj_n(x)\right]' - \mu j_n(x)\left[mxj_n(mx)\right]'}{m^2 j_n(mx)\left[xh_n^{(1)}(x)\right]' - \mu h_n^{(1)}(x)\left[mxj_n(mx)\right]'}, \\ b_n = \frac{\mu j_n(mx)\left[xj_n(x)\right]' - j_n(x)\left[mxj_n(mx)\right]'}{\mu j_n(mx)\left[xh_n^{(1)}(x)\right]' - h_n^{(1)}(x)\left[mxj_n(mx)\right]'}, \quad (3)$$

where $x = kR$, $j_n(x)$ and $y_n(x)$ are the spherical Bessel function of the first kind and the spherical Neumann function, respectively, and $h_n^{(1)}(x)$ is the spherical Hankel function of the first kind. $k = \omega\sqrt{\varepsilon_{PDMS}}/c$ is the wavenumber, c is the speed of light, $m = \sqrt{\varepsilon_{TiN}/\varepsilon_{PDMS}}$, and $\varepsilon_{PDMS} \equiv \varepsilon_{PDMS}(\omega) \approx 1.96$ [17] and $\varepsilon_{TiN} \equiv \varepsilon_{TiN}(\omega)$ are the dielectric function of PDMS and TiN, respectively. The dielectric function of TiN is obtained by fitting experimental data over a wide range of frequency with a generalized Drude-Lorentz model [22], which is

$$\varepsilon_{TiN}(\omega) = \varepsilon_\infty - \frac{\omega_p^2}{\omega(\omega + i\Gamma_D)} + \sum_{j=1}^{2} \frac{\omega_{L,j}^2}{\omega_{0,j}^2 - \omega^2 - i\gamma_j\omega}, \tag{4}$$

where $\varepsilon_\infty = 5.18$ is the permittivity at infinite frequency, $\omega_p \approx 7.38$ eV is the plasma frequency and $\Gamma_D \approx 0.26$ eV is the damping parameter in the Drude model or the second term in Eq. (4). The third term in Eq. (4) corresponds to the Lorentz model with parameters: $\omega_{L,1} \approx 6.5$ eV, $\omega_{L,2} = 1.5033$ eV, $\omega_{0,1} = 4.07$ eV, $\omega_{0,2} = 2.02$eV, $\gamma_1 = 1.42$ eV, and $\gamma_1 = 1.42$ eV [22].

From Eqs. (2-4), one can determine the effective absorption coefficient by using the BeerLambert law,

$$\alpha = NQ_{ext} = \frac{3\Phi Q_{ext}}{4\pi R^3}, \tag{5}$$

where N is the density number of particles.

The random dispersion of TiN nanoparticles in PDMS allows us to use the effective medium approximation [21] to estimate the thermal conductivity and mass density as

$$\begin{aligned} K_d &= K_{PDMS}(1-\Phi) + K_{TiN}\Phi, \\ \rho_d &= \rho_{PDMS}(1-\Phi) + \rho_{TiN}\Phi, \\ c_d &= c_{PDMS}(1-\Phi) + c_{TiN}\Phi, \end{aligned} \tag{6}$$

where $\Phi = N4\pi R^3/3$ is the volume fraction of particles, $K_{PDMS} = 0.16$ W/m/K, $K_{TiN} = 60$ W/m/K, $\rho_{PDMS} = 970$ kg/m^3, $\rho_{TiN} = 5400$ kg/m^3, $c_{PDMS} = 1460$ J/kg/K, $c_{TiN} = 533$ J/kg/K [17].

3. Results and discussions

To validate our theoretical approach in the previous section, we compare theoretical predictions and experimental data of temperature increase of ultra-flexible metamaterials under 808-nm laser illumination at the laser intensity of 6000 W/cm^2. Figure 2 shows the time dependence of surface temperature rise ($z = 0$) given by theory and experiment in Ref. [17]. Since the volume fraction is found to be $\Phi = 1.2 \times 10^{-3}$, the average interparticle separation distance is approximately $15R$ which is sufficiently large for us to ignore interference of electromagnetic fields among TiN nanoparticles. Thus, our theoretical framework is completely valid. Furthermore, our calculations agree well with experimental data (as seen in Fig. 2). These theoretical results are provided without any adjustable parameter. For this reason, our approach is reliably predictive.

Note that our model and other simulations [23, 24, 25] use constant values for the thermal conductivity, mass density, and specific heat capacity during the heating process. This assumption may be true for TiN but PDMS is a polymer and its properties are sensitive to temperature. Particularly, the temperature rise is larger than 50 K after 300s of laser irradiation. This thermal variation is large enough to cause some changes in properties of polymer. Howeve, the relatively quantitative theory-experiment accordance in Fig. 2 suggests that the temperature dependence of K_d, ρ_d, and c_d induces secondary effects on the photothermal heating.

To investigate how the particle density affects the photothermal heating, we calculate the temperature rise at the hottest spot ($z = r = 0$) at $t = 300s$ as a function of volume fractions

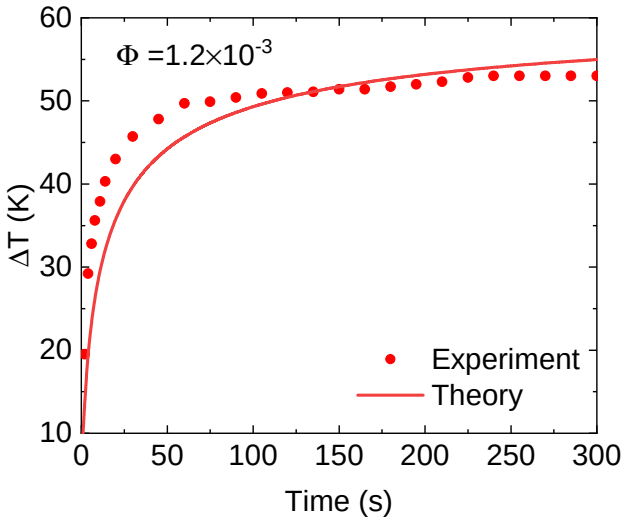

Figure 2. (Color online) Time dependence of the temperature rise at the surface of ultra-flexible metamaterials with $\Phi = 1.2 \times 10^{-3}$ of 30-nm TiN nanoparticles under 808-nm laser irradiation at the laser intensity of 6000 W/m^2.

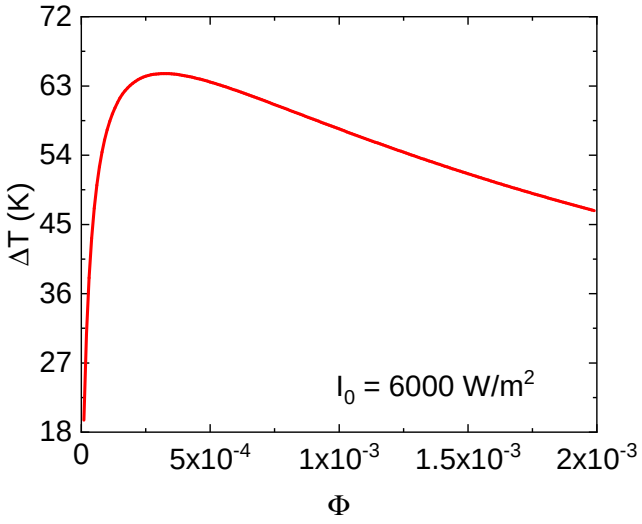

Figure 3. (Color online) The temperature rise at the surface of ultra-flexible metamaterials at $t = 300$ s as a function of volume fraction of 30-nm TiN nanoparticles under 808-nm laser irradiation at the laser intensity of 6000 W/m^2.

of TiN particles and show numerical results in Fig. 3. Φ remains still to be low to ensure no occurrence of plasmonic coupling. Interestingly, $\Delta T(r = z = 0)$ varies in a non-monotonic manner. When $\Phi \leq 2.5 \times 10^{-4}$, mixing more TiN particles into PDMS significantly increases the light absorption of the metamaterials. Thus, one can see an increase of $\Delta T(r = z = 0)$ up to 64 K at $\Phi = 2.5 \times 10^{-4}$. However, continuing to increase the density of particle, as seen in Eq. (6), the thermal conductivity is increased due to $K_{TiN} > K_{PDMS}$. Thus, the thermal dissipation becomes significantly easier and this leads to a decrease of $\Delta T(r = z = 0)$ when $\Phi > 2.5 \times 10^{-4}$. It is essential to know a critical value of Φ which maximizes the hottest spot to optimize the photothermal performance of the systems. This optimization is strongly dependent on not only the particle density, but also the particle size.

When we replace the above incident light with the AM1.5 solar light, the spatial distribution of the ultra-flexible metamaterial can be calculated using [19]

$$\begin{aligned}\Delta T(r,z,t) &= \int_{\lambda_{min}}^{\lambda_{max}} \frac{E_\lambda \alpha}{2\rho_d c_d} d\lambda \int_0^t \exp\left(-\frac{\beta^2 r^2}{1+4\beta^2\kappa t'}\right) \frac{e^{\alpha^2 \kappa t'}}{1+4\beta^2\kappa t'} \times \\ &\times \left[e^{-\alpha z}\mathrm{erfc}\left(\frac{2\alpha\kappa t' - z}{2\sqrt{\kappa t'}}\right) + e^{\alpha z}\mathrm{erfc}\left(\frac{2\alpha\kappa t' + z}{2\sqrt{\kappa t'}}\right)\right] dt', \end{aligned} \quad (7)$$

where E_λ is the global solar spectrum, the lower and upper limit of this integral are $\lambda_{min} = 280$ nm and $\lambda_{max} = 3000$ nm corresponding to the minimum and maximum wavelength of the incident solar radiation, respectively.

Figure 4a shows the solar-induced time evolution of the hottest spot on the metamaterials ($\Delta T(r = z = 0, t) \equiv \Delta T$) at $\Phi = 1.2 \times 10^{-3}$. In these calculations, we suppose that the spot size of the solar radiation does not change in comparison with the 808-nm laser light above. During the irradiation, a monotonic increase of $\Delta T(r = z = 0, t)$ behaves in the same manner as the case of laser illumination as shown in Fig. 2. However, within 300s, ΔT grows approximately 9.4 K, which is 6 times less than the laser-induced heating (seen in Fig. 2). Note that the intensity of AM1.5 solar simulator is $\int_{\lambda_{min}}^{\lambda_{max}} E_\lambda d\lambda \approx 1000$ W/m^2. Meanwhile, interestingly the laser intensity used for calculations in Fig. 2 is 6000 W/m^2 that is 6 times greater than the solar intensity. This finding suggests that the absorption of 30-nm TiN particle at 808 nm is equivalent with the average absorption of the particle over the solar spectrum frequency range.

An increase of Φ from 10^{-5} to 2×10^{-3} leads to a decrease of $\Delta T(z = r = 0, t = 300s)$ due to enhancement of thermal conductivity. Again, this enhancement facilitates the thermal dissipation although the absorbed energy increases. To quantitatively determine the variation, we carry out calculations and show numerical results in Fig. 4b. We find that the temperature rise decreases from 13 K to 8 K. The reduction of $T(z = r = 0, t)$ as increasing Φ is similar to results in Fig. 2 but the critical value of Φ, which $\Delta T(z = r = 0, t = 300s)$ is maximized, is shifted to a small range.

It seems that the largest temperature rise of the metamaterials under solar irradiation is less than 13 K. Equation (7) allows us to determine contribution of each range of wavelength to the photothermal heating. The fact that polymer's properties may slightly change with temperature in this thermal range. Thus, assumptions in our approach become more accurate. One could expect that theoretical predictions have better quantitative agreement with experiments. However, UV radiation can break bonding in polymers and lead to degradation. Thus, solar-induced aging effects should be considered as a factor to deviate theory and experiment if the devices work outside for a sufficiently long time.

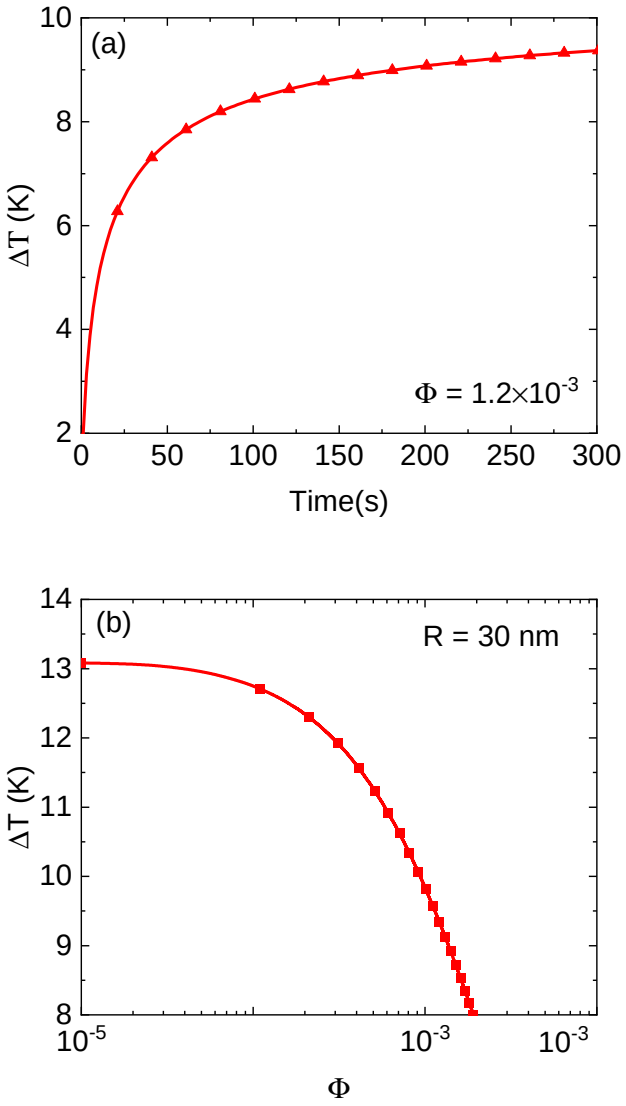

Figure 4. (Color online) (a) Time dependence of the hottest spot on the surface of the ultra-flexible metamaterial irradiated by a solar spectrum at $\Phi = 1.2 \times 10^{-3}$. (b) The solar-induced temperature rise at $t = 300s$ as a function of Φ.

4. Conclusions

We have shown a theoretical approach to describe the temperature rise of TiN-PDMS composites as irradiated by laser and solar light. Under illumination of 808-nm laser, our theoretical predictions agree well with experiments in Ref. [17]. This is advancement of the model compared to others since the quantitative agreement is obtained without adjustable or fitting parameters. When the particle volume fraction increases from 0 to 2.5×10^{-4}, more optical energy is absorbed by TiN nanoparticles and it leads to an increase of ΔT. Beyond the critical value of Φ, the absorbed optical energy is still grows but the thermal conductivity of TiN-PDMS mixtures also increases. A growth of the thermal conductivity facilitates the heat transfer in the studied systems and reduces the temperature rise. The nonmotononic variation of ΔT as increasing Φ suggests us how to maximize the photothermal heating. From this, we can find an appropriate

density of particles to design plasmonic devices to lower cost but remain the heating performance. When the incident light is solar, the temperature rise is much smaller than the case of laser light. This is obvious since the intensity of AM 1.5 solar light is 1000 W/m^2, which is 6 times less than the laser intensity. The solar- and laser-induced temperature rise could be the same if they are operated at the same intensity. Interestingly, the nonmonotonic behavior of ΔT with Φ is still held. But the critical Φ that obtains a maximum temperature is approximately 10^{-5}. This implies that using light source with a wide range of wavelength could reduce the critical Φ and design plasmonic devices with the equivalent heating performance but use a smaller density of plasmonic nanoparticles.

Acknowledgments
This research is funded by Vietnam Academy of Science and Technology under grant number KHCBVL.05/22-23.

References
[1] Lal S, Clare S E and Halas N J 2008 *Acc. Chem. Res.* **41** 1842
[2] Kim M, Lee J H and Nam J M 2019 *Adv. Sci.* **6** 1900471
[3] Boriskina S V, Ghasemi H and Chen G 2013 *Mater. Today* **16** 375
[4] Furube A and Hashimoto S 2017 *NPG Asia Materials* **9** e454
[5] Wang Y, Zhang J, Liang W, Yang H, Guan T, Zhao B, Sun Y, Chi L and Jiang L 2022 *CCS Chem.* **4** 1153
[6] Tanzid M, Sobhani A, DeSantis C J, Yao Cui, Hogan N J, Samaniego A, Veeraraghavan A and Halas N J 2016 *PNAS* **113** 5558
[7] Willets K A, Wilson A J, Sundaresan V and Joshi P B 2017 *Chem. Rev.* **117** 7538
[8] Kim J M, Lee C, Lee Y, Lee J, Park S J, Park S and Nam J M 2021 *Adv. Mater.* **33** 2006966
[9] Wang L, Kafshgari M H and Meunier M 2020 *Adv. Funct. Mater.* **30** 2005400
[10] Yu H, Peng Y, Yang Y and Li Z Y2019*npj Comput. Mater.* **5** 45
[11] Naik G V, Shalaev V M and Boltasseva A 2013 *Adv. Mater.* **25** 3264
[12] Naik G V, Kim J and Boltasseva A 2011 *Opt. Mater. Express* **1** 1090
[13] Sugavaneshwar R P, Ishii S, Dao T D, Ohi A, Nabatame T and Nagao T 2018 *ACS Photonics* **5** 814
[14] GulerU, Kildishev A V, Boltasseva A and Shalaev V M 2015 *Faraday Discuss.* **178** 71
[15] Naik G V, Schroeder J L, Ni X, Kildishev A V, Sands T D and Boltasseva A 2012 *Opt. Mater. Express* **2** 478
[16] Yick S, Murdock A T, Martin P J, Kennedy D F, Maschmeyer T and Bendavid A 2018 *Nanoscale* **10** 7566
[17] Wang B, Jing Z, Zhao M, Yu P, Ashalley E, Li P, Ma C, Tong X, Caputo R, Govorov A O, Xu H and Wang Z M 2022 *Adv. Optical Mater.* 2200168
[18] Zhang H, Feng L, Liang Y and Xu T 2019 *Nanoscale* **11** 437
[19] Phan A D, Le N B, Nghiem T H L, Woods L M, Ishii S and Wakabayashi K 2019 *Phys. Chem. Chem. Phys.* **21** 19915
[20] Bartholomeusz B J 1988 *J. Appl. Phys.* **64** 3815
[21] Bohren C F and Huffman D R 1988 *Absorption and Scattering of Light by Small Particles* (Wiley, Weinheim, Germany)
[22] Reddy H, Guler U, Kudyshev Z, Kildishev A V, Shalaev V M and Boltasseva A 2017 *ACS Photonics* **4** 1413
[23] https://www.comsol.com/
[24] https://www.3ds.com/products-services/simulia/products/cst-studio-suite/
[25] https://www.ansys.com/